

# 7T versus 3T MR Angiography to Assess Unruptured Intracranial Aneurysms

Eva Leemans , Bart Cornelissen , M. L. C. Sing, Marieke Sprengers , Rene van den Berg , Yvo Roos , W. Pieter Vandertop , Cornelius Slump , Henk Marquering , and Charles Majoie 

From the Department of Biomedical Engineering & Physics, Amsterdam UMC, University of Amsterdam, Amsterdam, the Netherlands (EL, BC, MLC, HM); Department of Radiology and Nuclear Medicine, Amsterdam UMC, University of Amsterdam, Amsterdam, the Netherlands (EL, MS, R, HM, CM); MIRA Institute for Biomedical Engineering and Technical Medicine, University of Twente, Enschede, the Netherlands (BC, CS); Department of Neurology, Amsterdam UMC, University of Amsterdam, Amsterdam, the Netherlands (YR); and Neurosurgical Center Amsterdam, Amsterdam UMC, University of Amsterdam, Amsterdam, the Netherlands (WPV).

## ABSTRACT

**BACKGROUND AND PURPOSE:** Aneurysm size and neck measurements are important for treatment decisions. The introduction of 7T magnetic resonance angiography (MRA) led to new possibilities assessing aneurysm morphology and flow due to the higher signal-to-noise ratio. However, it is unknown if the size measurements on 7T MRA are similar to those on the standard 3T MRA. This study aimed to compare aneurysm size measurements between 7T and 3T MRA.

**METHODS:** We included 18 patients with 22 aneurysms who underwent both 3T and 7T MRA. Three acquisition protocols were compared: 3T time of flight (TOF), 7T TOF, and 7T contrast-enhanced MRA. Each aneurysm on each protocol was measured by at least two experienced neuroradiologists. Subsequently, the differences were evaluated using scatterplots and the intraclass correlation coefficients (ICC) of agreement.

**RESULTS:** There was a good agreement among the neuroradiologists for the height and width measurements (mean ICC: .78-.93); the neck measurements showed a moderate agreement with a mean ICC of .57-.72. Between the MR acquisition protocols, there was a high agreement for all measurements with a mean ICC of .81-.96. Measurement differences between acquisition protocols (0-2.9 mm) were in the range of the differences between the neuroradiologists (0-3.6 mm).

**CONCLUSION:** Our study showed that 7T MRA, both nonenhanced and contrast-enhanced, has a high agreement in aneurysm size measurements compared to 3T. This suggests that 7T is useful for reliable aneurysm size assessment.

**Keywords:** Aneurysms, MR angiography, size measurements, ultra-high field MRI.

**Acceptance:** Received May 10, 2020, and in revised form July 24, 2020. Accepted for publication August 3, 2020.

**Correspondence:** Address correspondence to Eva Leemans, Departments of Biomedical Engineering and Physics, Radiology and Nuclear Medicine, Academic Medical Center, University of Amsterdam, Meibergdreef 9, 1105AZ, Amsterdam, the Netherlands. E-mail: e.l.leemans@amsterdamumc.nl.

**Acknowledgments and Disclosure:** This study was supported by a grant from the TWIN association, Hengelo, the Netherlands. René van den Berg—Unrelated: Consultancy: Codman Depuy Neurovascular, Comments: coil development,\* Henk Marquering—Other Relationships: cofounder and shareholder of Nico-lab. Charles Majoie—Related: Grant: TWIN Foundation\*; Unrelated: Grants/Grants Pending: Dutch Heart Foundation, Stryker\*, Other Relationships: shareholder of Nico-lab. \*Money paid to the institution.

J Neuroimaging 2020;30:779-785.  
DOI: 10.1111/jon.12772

## Introduction

An increasing number of unruptured intracranial aneurysms are detected due to the increase in brain imaging.<sup>1</sup> To prevent aneurysm rupture, which carries a high morbidity and mortality,<sup>2</sup> the aneurysm can be obliterated from the normal circulation by surgical clipping or several endovascular options (eg, coiling or flow diverter placement). As treatment is not risk-free, the treatment decision is based on both the treatment and rupture risk.

Currently, the rupture risk estimation is primarily based on aneurysms size, shape, and location and patient characteristics (age, ethnicity, and earlier subarachnoid hemorrhage).<sup>3</sup> Larger aneurysm sizes have shown to have a higher risk of rupture.<sup>4,5</sup> The difficulty of the treatment also depends on aneurysm size, shape, and location. Additionally, the aneurysm neck size has a large influence on treatment complexity.<sup>6</sup> A neck diameter smaller than the dome size greatly increases the chance of full occlusion after treatment with coiling. Thus, for both the rup-

ture risk and treatment risk, it is important to accurately assess the size of the aneurysm and its neck. Consequently, incorrect measurements could lead to a suboptimal treatment decision.

Time-of-flight (TOF) MR angiography (MRA) at 3 tesla (3T) is the imaging modality of choice for evaluation of unruptured intracranial aneurysms.<sup>7</sup> The advantages of this method are that it is radiation free, has no need of contrast medium administration, and has a high spatial resolution. Advances in software and hardware have made 7 tesla (7T) MRI systems available for clinical purposes. This higher field strength, compared to the regular 3T systems, results in an increased signal-to-noise ratio, which facilitates acquisition at higher resolutions.<sup>8,9</sup> Several sequences already showed to benefit from high-field strengths, such as phase contrast imaging<sup>10</sup> and vessel wall imaging.<sup>11,12</sup>

Previous studies evaluated the image quality of TOF MRA, showing improved image quality with increasing magnetic field strengths. For instance, Von Morze et al showed improved

This is an open access article under the terms of the Creative Commons Attribution-NonCommercial License, which permits use, distribution and reproduction in any medium, provided the original work is properly cited and is not used for commercial purposes.

visualization of the intracranial vasculature at 7T, especially of the smaller peripheral vessels.<sup>13</sup> However, 7T MR systems have more transmit field inhomogeneities causing artifacts, which might lead to inaccurate aneurysm measurements on 7T MRI.

As it is still unclear whether aneurysm measurements on 7T are comparable to measurements on 3T, the goal of this study was to assess the agreement in manual aneurysm measurements at 3T and 7T MRA in unruptured and untreated intracranial aneurysms. We chose to include both nonenhanced and enhanced 7T MRA to give a full overview of the possibilities.

## Methods

### Study Population

This study included patients with an unruptured intracranial aneurysm with repeated imaging during regular follow-up, who participated in the “Improving risk prediction of intracranial aneurysms (IMPRES)”-study. The study was approved by the local IRB, and all patients signed an informed consent form. The included patients participated in the study between October 2016 and December 2018 and were at least 18 years old. Patients with contraindications for the 7T MRI or a poor renal clearance (lower than 30 mL/min) were excluded. During this time period, we identified 160 consecutive patients, 12 were excluded due to poor quality of the follow-up imaging, 82 had contraindications for 7T MR, 11 were in a too poor clinical condition for additional imaging, and 37 did not want to participate. In total, 18 patients with 22 aneurysms were included.

### Imaging

The 3T MRA was part of the regular clinical work-up. Both 3T and 7T MRA's were made on a Philips medical systems scanner (Philips healthcare, Best, the Netherlands). 3T scanning was done on an Ingenia System with a multichannel head coil. 3T acquisition was according to the multiple overlapping thin slab acquisition (MOTSA) technique with sensitivity encoding (SENSE, acceleration factor = 5). Scan parameters were; matrix: 512\*512, repetition time (TR): 20.4-25.0 milliseconds, echo time (TE): 3.5-4.1 milliseconds, field of view: 512\*512, and flip angle 20°. The 3T data were acquired and constructed at a resolution of .35-.39 mm (anterior-posterior), .35-.39 mm (right-left), and .5 mm (superior-inferior). This resulted in a total scan-time of 5.5 minutes. 7T imaging was done using an Achieva system and a transmit head coil with 32-channel receiving elements (Nova Medical, Wilmington, MA). 7T acquisition used a TOF with SENSE protocol (acceleration factor = 5). Scan parameters for the 7T scan were; matrix: 1,008\*1,008, TR: 12.7-16.3 milliseconds, TE: 2.3-2.6 milliseconds, field of view: 1,008\*1,008, and flip angle 25°. The 7T data were acquired at a resolution of .19 mm (anterior-posterior), .19 mm (right-left), and .5 mm (superior-inferior) and reconstructed to a similar resolution as the 3T-imaging of .5 mm (anterior-posterior), .5 mm (right-left), and .5 mm (superior-inferior). This resulted in a total scan-time of 4 minutes. A second 7T MRA with the same scan settings was made after the administration of .1 mL/kg Gadovist (1 mmol/mL) or .2 mL/kg Dotarem (.5 mmol/mL). No contrast-enhanced MRA was done on 3T as this scan was part of regular-clinical follow-up, while the 7T was done for research purposes.

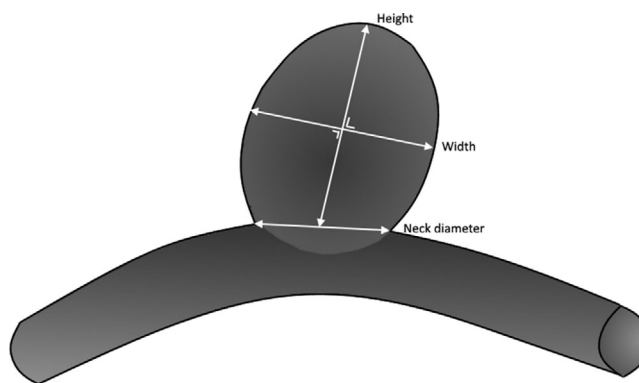


**Fig 1.** Definition of the aneurysm size measurements.

### Size Assessment

Three neuroradiologists, with each more than 10 years of experience, evaluated the 3T MRA and 7T nonenhanced and enhanced MRAs. Each neuroradiologist measured all the aneurysms at two MRA acquisition protocols, using multiplanar reconstruction within Impax (Agfa Healthcare, Germany). All measurements were done on the 2D images. At least two neuroradiologists measured each aneurysm for each MRA acquisition protocol. The neuroradiologists were blinded to the measures by the other radiologists and to their own measurements between acquisition protocols. Scans were first qualitatively evaluated on image quality using a four-point scale: (1. Poor, not diagnostically useful; 2. Moderate [aneurysm can be seen but is hard to delineate]; 3. Good [aneurysm can be completely delineated]; and 4. Excellent [aneurysm and surrounding vessels can be clearly seen and delineated]). Subsequently, for each aneurysm, the height, width, and neck diameter were measured. No measurements were performed on aneurysm images with a poor image quality (score of 1), given five times in three different aneurysms (all nonenhanced 7T MRAs). Measurements were done for the images with a moderate quality score of 2, given six times in four aneurysms (four times for a 3T MRA, one time in a nonenhanced 7T MRA, and one time in a contrast-enhanced 7T MRA). The following definitions were used:<sup>14</sup> the neck diameter is the largest diameter measured where the aneurysm deviates from the parent vessel, the maximal height is the maximal distance between the aneurysm neck and aneurysm fundus tip, the maximal width is the maximal size of the aneurysm measured perpendicular to the height measurements, see Figure 1.

### Statistics

We compared the aneurysm measurements between each neuroradiologist and between each acquisition protocol. First, scatterplots were made to visualize agreement. Second, Bland-Altman analyses were performed determining the bias and limits of agreement (LoA) for each comparison. Subsequently, the intraclass correlation coefficients (ICCs) were calculated to determine the agreement between the measurements of the neuroradiologists and between MRA acquisition protocols. An ICC of 1 indicates perfect agreement, and an ICC of 0 shows no agreement.

Table 1. Average Measurements and Standard Deviation Per MRA Acquisition Protocol

	Measurements Mean $\pm$ SD/Median (range)			Bland-Altman analysis Mean (95% CI)		
	3T	7T	7T-CE	3T and 7T	3T and 7T-CE	7T and 7T-CE
Quality (mean (range))	3 (2-3)	3 (1-4)	4 (1-4)			
Height (mm)	4.8 $\pm$ 1.9	4.8 $\pm$ 1.8	4.6 $\pm$ 2.0	-3 (-2.1 to 1.5)	.3 (-1.5 to 2.1)	.0 (-2.0 to 2.0)
Width (mm)	4.9 $\pm$ 2.3	4.9 $\pm$ 2.6	4.7 $\pm$ 2.5	-3 (-2.9 to 2.3)	.2 (-2.0 to 2.4)	.2 (-1.2 to 1.4)
Neck (mm)	3.5 $\pm$ 1.7	3.7 $\pm$ 1.9	3.3 $\pm$ 1.8	-1 (-1.5 to 1.3)	.1 (-1.7 to 1.9)	-2 (-2.4 to 2)

3T, 3 tesla nonenhanced MRA; 7T, 7 tesla nonenhanced MRA; 7T-CE, 7 tesla contrast-enhanced MRA; SD, standard deviation; CI, confidence interval.

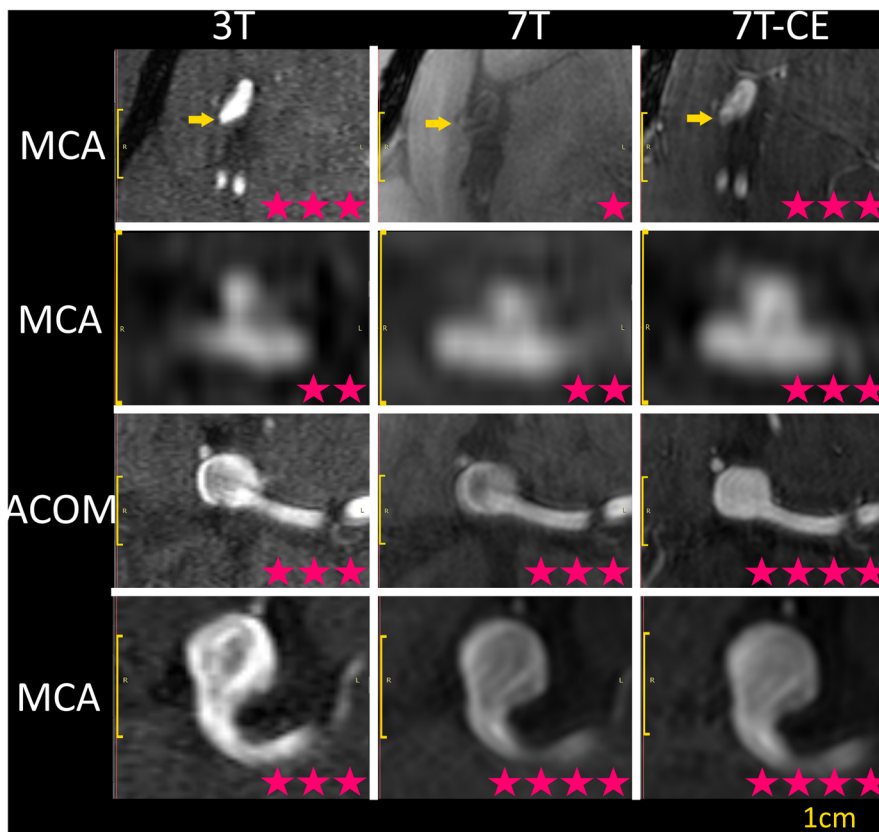


**Fig 2.** Examples of poor (1 star), moderate (2 stars), good (3 stars), and excellent (4 stars) image quality MRIs. Each row shows a different aneurysm, and each column shows a different acquisition protocol. The yellow bar (10 mm) shows the scale for each scan. The top row shows a middle cerebral artery aneurysm (yellow arrow), with a poor quality on the nonenhanced 7T (middle). In this case, the poor quality was due to the inhomogeneous b1-field. Note: Images were created using a DICOM-viewer with image interpolation, interpolation was turned off during scoring. MCA, middle cerebral artery; ACOM, anterior communicating artery; CE, contrast-enhanced.

All statistical analyses were performed with R-studio (version 1.1.456). A *P*-value of .05 was considered statistically significant.

## Results

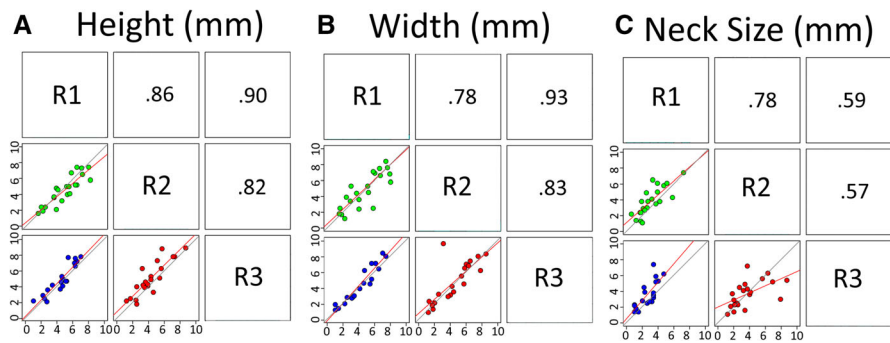
The average age at time of the reference 3T MRA of the 18 patients was 62 years (range 48-76). Three patients had multiple aneurysms. The maximum aneurysm size was 1.5-11 mm. Aneurysm locations were at the middle cerebral artery (*n* = 11, 50%), anterior communicating artery (*n* = 4, 18%), internal carotid artery (ICA, *n* = 3, 14%), and basilar artery (*n* = 2, 9%). The average time between the 3T and 7T imaging was 114 days (range 34-217 days).

Table 1 shows the quality scores and the measurements for each MRA acquisition protocol. The quality of the 7T MRA,

especially the nonenhanced MRA, varied substantially among patients. While the 3T MRA mostly had a good and in some cases moderate (*n* = 2, 5%) image quality, the image quality of three of the nonenhanced 7T MRAs was classified as poor and for six cases, the image quality was classified as excellent by all observers. An example of an excellent and poor-quality scan can be seen in Figure 2. The 7T contrast-enhanced MRAs most often showed an excellent quality (*n* = 21, 50%), compared to the 3T (*n* = 0, 0%) and nonenhanced 7T (*n* = 7, 16%), but two intracavernous ICA aneurysms were difficult to measure due to contrast-enhancement within the cavernous sinus.

### Scatterplots and Intraclass Correlation Coefficient

The scatterplots, as depicted in Figures 3 and 4, show similar aneurysm sizes as measured by the neuroradiologists.



**Fig 3.** Scatterplots and correlation matrices comparing measurements by three neuroradiologists. The plots in the right upper corner show the intraclass correlation coefficients, the plots in the lower left corner show the scatterplots with the linear trend (red) and identity line (gray). The axes show the size in mm. R1, first neuroradiologist; R2, second neuroradiologist; R3, third neuroradiologist. [Color figure can be viewed at wileyonlinelibrary.com]

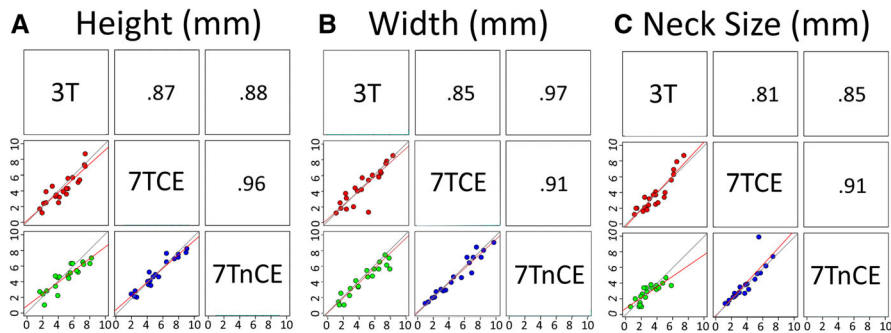


**Fig 4.** Scatterplots and correlation matrices comparing three acquisition protocols. The plots in the right upper corner show the intraclass correlation coefficients, the plots in the lower left corner show the scatterplots with the linear trend (red) and identity line (gray). The axes show the size in mm. 3T, 3 tesla nonenhanced MRA; 7TCE, 7T contrast-enhanced MRA; 7TnCE, 7T nonenhanced MRA. [Color figure can be viewed at wileyonlinelibrary.com]

Table 2. Interclass Correlation Matrix with 95% Confidence Intervals for between Neuroradiologists and MRA Acquisition Protocols

	Neuroradiologist			MRA acquisition protocol		
	R1 and R2	R2 and R3	R1 and R3	3T and 7T	3T and 7T	7T and 7T-CE
Height	.86 (.68-.94)	.82 (.53-.93)	.90 (.74-.96)	.87 (.7-.95)	.96 (.89-.98)	.88 (.74-.95)
Width	.78 (.55-.90)	.83 (.63-.93)	.93 (.83-.97)	.85 (.67-.94)	.91 (.8-.96)	.97 (.92-.99)
Neck	.72 (.33-.88)	.57 (.18-.80)	.59 (.06-.84)	.81 (.59-.92)	.91 (.65-.94)	.85 (.79-.96)

R1, first neuroradiologist; R2, second neuroradiologist; R3, third neuroradiologist; 3T, 3 tesla nonenhanced MRA; 7T, 7 tesla nonenhanced MRA; 7T-CE, 7 tesla contrast-enhanced MRA.

The agreement for the height and width measurements was good with a mean ICC of .78-.93. The neck measurements show a moderate agreement with a mean ICC of .57-.72. All ICC-values of agreement and their confidence intervals are shown in Table 2. For the MRA acquisition protocols, the scatterplots also show a high similarity. For all measurements, the agreement was good to high with a mean ICC of .81-.92. A clear linear association without any outliers was seen between the measurements of each acquisition protocol.

#### Bland-Altman Analysis

The Bland-Altman analyses showed an average difference in height between neuroradiologists of .4 mm (with LoA ranging from -2.2 to 2.6), see Table 3. The largest difference was seen in

the neck diameter between the first and third neuroradiologist (on average -1.1 mm, LoA: -3.3 to 1.1). The Bland-Altman plots did not show clear trends when comparing the differences to the average measurements between neuroradiologists; all plots are shown in Figure 5.

For the comparisons between MRA acquisition protocols, see Table 1, the Bland-Altman analyses showed differences between 3T and 7T of on average -3 mm (LoA: -2.1 to 1.5 mm), -3 mm (LoA: -2.9 to 2.3 mm), and -1 mm (LoA: -1.5 to 1.3 mm) for the height, width, and neck, respectively. These differences and LoA between image acquisition protocols were smaller compared to the differences within observers. For the MRA acquisition protocols, no clear trends or variability differences depending on the average size measurements were seen, see Figure 6.

Table 3. Average Measurements and Standard Deviation Per Neuroradiologist

	Measurements Mean ± SD			Bland-Altman analysis Mean difference (Limit of agreement)		
	R1	R2	R3	R1 and R2	R1 and R3	R2 and R3
Height (mm)	4.8 ± 1.8	4.4 ± 1.8	4.9 ± 2.0	-.4 (-2.2 to 1.4)	-.3 (-1.9 to 1.3)	.6 (-1.4 to 2.6)
Width (mm)	4.7 ± 2.3	4.9 ± 2.6	4.6 ± 2.6	.2 (-2.9 to 3.3)	-.3 (-1.9 to 1.3)	.3 (-2.8 to 3.4)
Neck (mm)	3.8 ± 1.9	3.8 ± 1.9	3.3 ± 1.7	.7 (-1.5 to 2.9)	-1.1 (-3.3 to 1.1)	-.1 (-3.6 to 3.5)

R1, first neuroradiologist; R2, second neuroradiologist; R3, third neuroradiologist; SD, standard deviation.

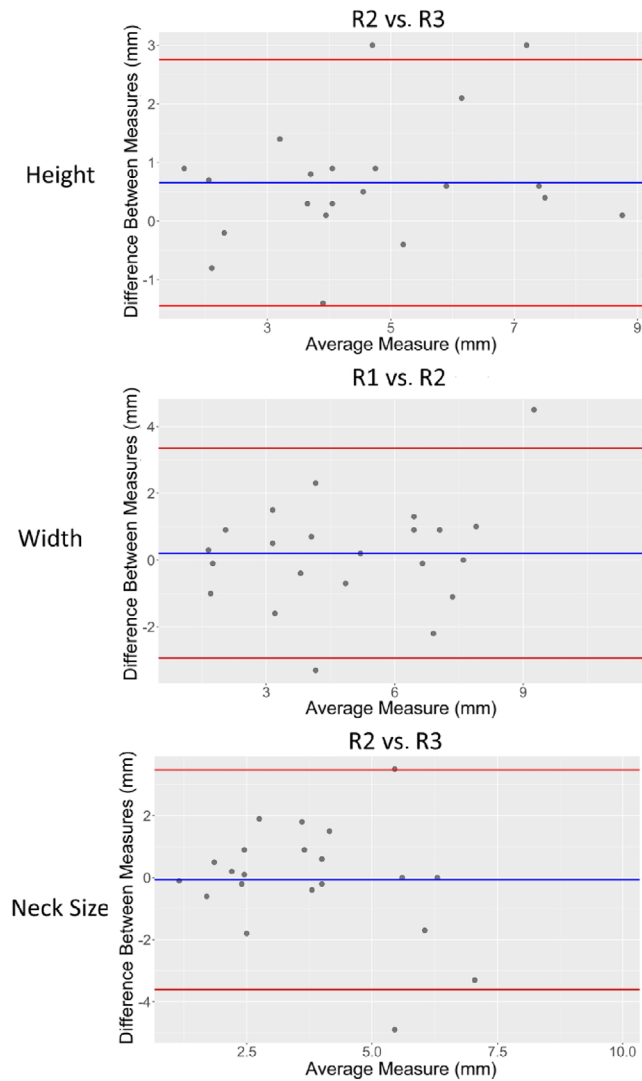


**Fig 5.** Bland-Altman plots comparing the differences in mm between neuroradiologists, showing the plot with the biggest difference for each measurement. R1, first neuroradiologist; R2, second neuroradiologist; R3, third neuroradiologist.

### Discussion

Our findings show that aneurysm height, width, and neck size measurements on 7T MRA in both nonenhanced and contrast-enhanced scans are comparable to 3T MRA. Although some differences were seen, these were smaller than the differences between neuroradiologists within single acquisitions. This suggests that 7T MRA is also suitable to use for treatment decisions.

Some nonenhanced 7T MR scans had a poor image quality, severely limiting the visualization of the aneurysm. This agrees

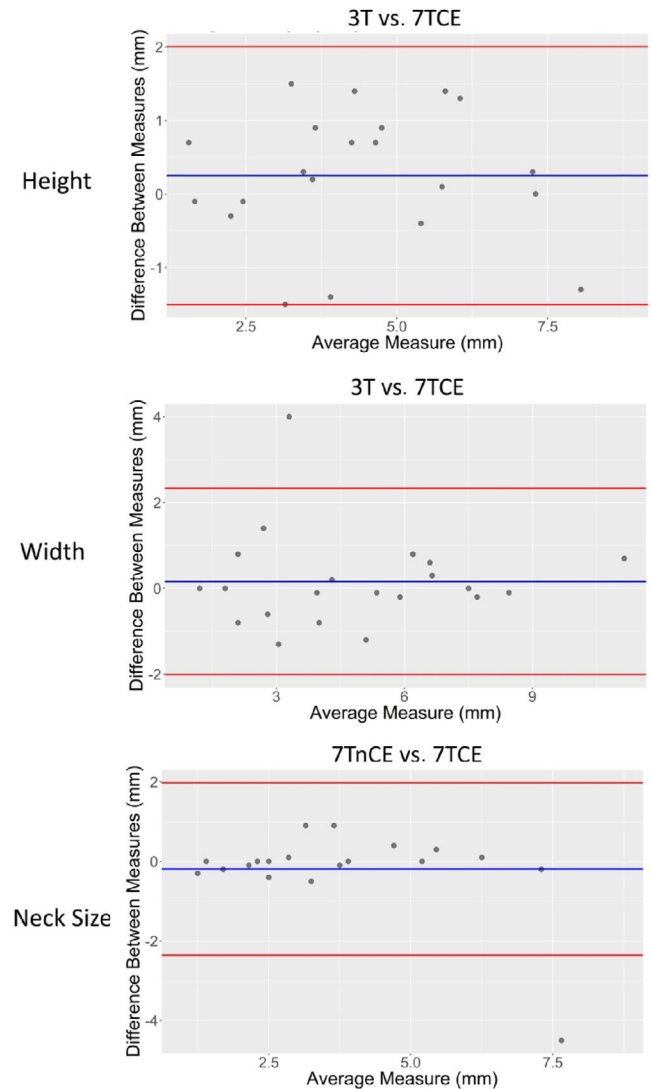


**Fig 6.** Bland-Altman plots comparing the differences in mm between MRI acquisition protocols, showing the plot with the biggest difference for each measurement. 3T, 3 tesla nonenhanced MRA; 7T, 7 tesla nonenhanced MRA; 7T-CE, 7 tesla contrast-enhanced MRA.

with observations of previous studies, the pulsatile blood flow is more susceptible to field inhomogeneities, which might result in signal loss.<sup>15</sup> This effect occurs most often in aneurysms closer to the temporal lobe as this area is mostly affected by signal loss due to the inhomogeneities. Additionally, the 7T MRA did not use a MOTSA technique, contrary to the 3T MRA. As a result, the 7T TOF images likely have more signal loss due to saturation effects. However, the use of this technique is still

limited on 7T MRI setups, and was not implemented at our 7T system. As 3T has been widely used for over 10 years, the available sequences and setup have been optimized for intracranial vessel and aneurysm assessment, which is also reflected by the consistently good image quality in our study. Further optimization still has to be done at 7T.<sup>16</sup> The introduction of multichannel coils should reduce field inhomogeneities by improving the B1-shimming.<sup>13,17,18</sup> Additionally, multicoil shimming also improves the B0-inhomogeneities.<sup>19</sup> This can further improve image quality, especially near the air-tissue interfaces, such as the sphenoid sinuses and mastoid. The 7T sequence used for this study was faster than the 3T sequence. Therefore, more time is available to either add other sequences—such as vessel wall imaging—or improve the resolution on 7T. However, the introduction of compressed sensing at 3T MRI also reduces the scanning time at 3T.<sup>20,21</sup>

For 7T imaging, we chose a similar reconstructed resolution to the 3T setup. Higher resolutions are possible with 7T, but this significantly increases the scanning time, increasing the possibility of the patient moving during the sequence. Higher resolutions and the increased sensitivity of 7T MRA especially benefit the visualization of the smaller arteries.<sup>9,22</sup> Small aneurysms (< 3 mm) can already be detected on 3T MRA.<sup>23</sup> The introduction of 7T, therefore, mostly benefits the assessment of small vascular structures and not aneurysm size assessment. Improved visualization of the vessels surrounding the aneurysm can be of great benefit in treatment planning. As a result, branches arising from the aneurysm could be easier identified on 7T MRA. Additionally, the complete aneurysm assessment also benefits from higher field strength, as phase contrast imaging<sup>10</sup> and vessel wall imaging<sup>11,12</sup> both showed improved visualization at higher field strengths.

The largest difference between 3T and 7T MRA was 2.9 mm. Nevertheless, the largest difference between the neuro-radiologists was 3.5. Thus, the differences between acquisition protocols are within normal ranges. These differences cannot be ignored. With a treatment threshold of 7 mm, a difference of 2 mm could result in a different treatment decision. In our study, we only had one case where the nonenhanced 7T MRA measured a height below 7 mm, while the 3T measurement was above 7 mm. Thus, in our population, these differences did not influence the treatment decision. However, such substantial differences, between neuro-radiologists and MRA acquisition protocols, will influence the assessment of aneurysm growth. In our study, measurements were done in a similar manner but within different sessions for each acquisition protocol. For growth assessment, it is recommended to simultaneously measure and compare the aneurysm size, as small deviations within the imaging plane may have a large influence on the measurements.

There are several limitations to this study. Although we found high agreement between the MRA acquisition protocols, this study is single center and single MR-manufacturer. The aneurysm size measurements might differ between scanner, due to the different settings and reconstruction algorithms. Another reason for size differences between the MRA acquisition protocols could be aneurysm growth, as the time between the scans was on average 114 days. However, we did not see growth on the available follow-up 3T MRA imaging (available in 16 of the 22 aneurysms), and thus this effect is negligible.

Due to the aneurysm characteristics, none of the aneurysm in our population were treated. As a result, the location of the

aneurysms included in this study did not represent the distribution observed in the general population. However, larger aneurysms at high-risk locations are more likely to be treated, and our cohort, therefore, represents the population that receives regular imaging.

The differences between neuro-radiologists in height and neck measurements were larger than the differences in width. As some aneurysms had a wide neck or vessels originating from the neck, the positioning of the neck by the neuro-radiologists differed. Some chose to position the plane below the branches, others chose to exclude the branches as this would likely be the plane chosen for aneurysm isolation during coiling or clipping. Since the aneurysm height was defined as the largest distance between the neck and aneurysm fundus, the height measurement also changed with the different neck plane positioning. Both of neck placements fit in the definition of Raghavan et al, which was used for the size measurements.<sup>14</sup>

The purpose of this study was not to compare the accuracy of aneurysm size measurements of the different MRA sequences used with the gold standard 3DRA, but to evaluate whether aneurysm size measurements on 7T scans are comparable to those performed on 3T scans. Therewith, time of flight MRA is the method of choice for regular aneurysm follow-up imaging due to its noninvasiveness. Previous studies showed a moderate to high agreement between measurements on 3T MRA and 3DRA imaging, but a low agreement was seen for the neck measurements.<sup>24-26</sup> As a result, an additional 3DRA should be made in cases where the neck measurements are crucial for the treatment decision.

To conclude, the results of our study showed that aneurysm morphology assessment at 7T MRA, both nonenhanced and contrast-enhanced, is comparable to nonenhanced 3T MRA assessment. Therefore, no additional 3T MRA is needed when imaging aneurysms for clinical or research purposes on 7T. As currently the quality of nonenhanced 7T MRA differs a lot between cases, we recommend further optimization of the 7T nonenhanced protocol or a contrast-enhanced MRA for aneurysms distal to the cavernous sinus. Aside from sequence optimization, other 7T sequences could also improve the image quality. For instance, at 7T, MPRAGE has shown better image quality and aneurysm delineation compared to nonenhanced TOF.<sup>27</sup> Additionally, other sequences could also profit from the high-field strength, such as phase contrast imaging<sup>10</sup> and vessel wall imaging.<sup>11,12</sup> As a result, a more complete assessment of the aneurysm can be made with 7T imaging.

## References

1. Vlak MH, Algra A, Brandenburg R, et al. Prevalence of unruptured intracranial aneurysms, with emphasis on sex, age, comorbidity, country, and time period: a systematic review and meta-analysis. *Lancet Neurol* 2011;10:626-36.
2. Rinkel GJ, Djibuti M, Algra A, van Gijn J. Prevalence and risk of rupture of intracranial aneurysms: a systematic review. *Stroke* 1998;29:251-6.
3. Greving JP, Wermer MJH, Brown RD, et al. Development of the PHASES score for prediction of risk of rupture of intracranial aneurysms: a pooled analysis of six prospective cohort studies. *Lancet Neurol* 2014;13:59-66.
4. UCAS Japan Investigators, Morita A, Kirino T, et al. The natural course of unruptured cerebral aneurysms in a Japanese cohort. *N Engl J Med* 2012;366:2474-82.

5. Morita A. Current perspectives on the unruptured cerebral aneurysms: origin, natural course, and management. *J Nippon Med Sch* 2014;81:194-202.
6. Songsaeng D, Geibprasert S, ter Brugge KG, et al. Impact of individual intracranial arterial aneurysm morphology on initial obliteration and recurrence rates of endovascular treatments: a multivariate analysis. *J Neurosurg* 2011;114:994-1002.
7. Thompson BG, Brown RD, Amin-Hanjani S, et al. Guidelines for the management of patients with unruptured intracranial aneurysms: a guideline for healthcare professionals from the American Heart Association/American Stroke Association. *Stroke* 2015;46:2368-400.
8. Balchandani P, Naidich TP. Ultra-high-field MR neuroimaging. *AJNR Am J Neuroradiol* 2015;36:1204-15.
9. Park C-A, Kang C-K, Kim Y-B, et al. Advances in MR angiography with 7T MRI: from microvascular imaging to functional angiography. *Neuroimage* 2018;168:269-78.
10. Van Ooij P, Zwanenburg JJM, Visser F, et al. Quantification and visualization of flow in the Circle of Willis: time-resolved three-dimensional phase contrast MRI at 7 T compared with 3 T. *Magn Reson Med* 2013;69:868-76.
11. Sato T, Matsushige T, Chen B, et al. Wall contrast enhancement of thrombosed intracranial aneurysms at 7T MRI. *AJNR Am J Neuroradiol* 2019;40:1106-11.
12. Kleinloog R, Korkmaz E, Zwanenburg JJM, et al. Visualization of the aneurysm wall: a 7.0-Tesla magnetic resonance imaging study. *Neurosurgery* 2014;75:614-22.
13. Von Morze C, Xu D, Purcell DD, et al. Intracranial time-of-flight MR angiography at 7T with comparison to 3T. *J Magn Reson Imaging* 2007;26:900-4.
14. Raghavan ML, Ma B, Harbaugh RE. Quantified aneurysm shape and rupture risk. *J Neurosurg* 2005;102:355-62.
15. Drangova M, Pelc NJ. Artifacts and signal loss due to flow in the presence of B<sub>0</sub> inhomogeneity. *Magn Reson Med* 1996;35:126-30.
16. Wrede KH, Johst S, Dammann P, et al. Improved cerebral time-of-flight magnetic resonance angiography at 7 Tesla—feasibility study and preliminary results using optimized venous saturation pulses. *PLOS One* 2014;9. <https://doi.org/10.1371/journal.pone.0106697>
17. Schmitter S, Wu X, Adriany G, et al. Cerebral TOF angiography at 7T: impact of B<sub>1</sub><sup>+</sup> shimming with a 16-channel transceiver array. *Magn Reson Med* 2014;71:966-77.
18. Madai VI, von Samson-Himmelstjerna FC, Sandow N, et al. Ultrahigh-field MPRAGE magnetic resonance angiography at 7.0T in patients with cerebrovascular disease. *Eur J Radiol* 2015;84:2613-7.
19. Stockmann JP, Wald LL. In vivo B<sub>0</sub> field shimming methods for MRI at 7 T. *Neuroimage* 2018;168:71-87.
20. Fushimi Y, Fujimoto K, Okada T, et al. Compressed sensing 3-dimensional time-of-flight magnetic resonance angiography for cerebral aneurysms. *Invest Radiol* 2016;51:228-35.
21. Fushimi Y, Okada T, Kikuchi T, et al. Clinical evaluation of time-of-flight MR angiography with sparse undersampling and iterative reconstruction for cerebral aneurysms. *NMR Biomed* 2017;30:e3774.
22. Nowinski WL, Puspitasaari F, Volkau I, et al. Comparison of magnetic resonance angiography scans on 1.5, 3, and 7 Tesla Units: a quantitative study of 3-dimensional cerebrovasculature. *J Neuroimaging* 2013;23:86-95.
23. Kapsalaki EZ, Rountas CD, Fountas KN. The role of 3 Tesla MRA in the detection of intracranial aneurysms. *Int J Vasc Med* 2012;2012:792834.
24. Mine B, Pezzullo M, Roque G, et al. Detection and characterization of unruptured intracranial aneurysms: comparison of 3T MRA and DSA. *J Neuroradiol* 2015;42:162-8.
25. Poethke J, Goubergrits L, Kertzsch U, et al. Impact of imaging modality for analysis of a cerebral aneurysm: comparison between CT, MRI and 3DRA. *IFMBE Proc* 2008;22:1889-93.
26. Ren Y, Chen G-Z, Liu Z, et al. Reproducibility of image-based computational models of intracranial aneurysm: a comparison between 3D rotational angiography, CT angiography and MR angiography. *BioMed Eng OnLine* 2016;15:50.
27. Wrede KH, Dammann P, Mönninghoff C, et al. Non-enhanced MR imaging of cerebral aneurysms: 7 Tesla versus 1.5 Tesla. *PLOS One* 2014;9:1-10.